Relativistic coupled-cluster-theory analysis of unusually large correlation effects in the determination of g_j factors in Ca^+

B. K. Sahoo[1,2,*] and Pradeep Kumar[1,3]

[1]*Atomic, Molecular and Optical Physics Division, Physical Research Laboratory, Navrangpura, Ahmedabad, Gujarat 380009, India*

[2]*State Key Laboratory of Magnetic Resonance and Atomic and Molecular Physics, Wuhan Institute of Physics and Mathematics, Chinese Academy of Sciences, Wuhan 430071, China*

[3]*Indian Institute of Technology Gandhinagar, Palaj, Gandhinagar, Gujarat 382355, India*

(Received 10 May 2017; published 17 July 2017)

We investigate roles of electron correlation effects in the determination of the g_j factors of the $4s\,^2S_{1/2}$, $4p\,^2P_{1/2}$, $4p\,^2P_{3/2}$, $3d\,^2D_{3/2}$, and $3d\,^2D_{5/2}$ states, representing different parities and angular momenta, of the Ca^+ ion. Correlation contributions are highlighted with respect to the mean-field values evaluated using the Dirac-Hartree-Fock method, relativistic second-order many-body theory, and relativistic coupled-cluster (RCC) theory with the single- and double-excitation approximation considering only the linear terms and also accounting for all the nonlinear terms. This shows that it is difficult to achieve results below 10^{-5} precision employing an approximate perturbative approach. We also find that contributions through the nonlinear terms and higher-level excitations such as triple excitations, estimated perturbatively in the RCC method, are found to be crucial to attain precise values of the g_j factors in the considered states of the Ca^+ ion.

DOI: 10.1103/PhysRevA.96.012511

I. INTRODUCTION

Spectroscopic studies of the singly ionized calcium (Ca^+) ion are of immense interest to both the experimentalists and theoreticians in many scientific applications. In particular, this ion is under consideration for a number of high-precision experimental studies such as in the atomic clock [1,2], quantum computation [3–5], and testing Lorentz symmetry violation [6]. A number of theoretical investigations have also been carried out in the determination of different physical quantities by employing a variety of many-body methods [7–14], which demonstrate the successful achievement of most of these properties meticulously compared to the experimental results.

On the other hand, there have been attempts to determine Landé g_j factors in the atomic systems to ultrahigh accuracy [7,15–17]. The main motivation of these studies was to test the validity of both the theories and measurements. Mostly atomic systems with few electrons are considered in these investigations, aiming to determine the role of higher-order quantum electrodynamics (QED) effects [17]. In these systems, both the QED and electron correlation effects contribute equally to match the theoretical calculations with the experimental results. Comparatively, only a few attempts have been made to reproduce the experimental values of the g_j factors to very high precision in the many-electron systems [7,15]. In the neutral or singly ionized heavy atomic systems, the electron correlation effects play a dominant role in estimating accurately the g_j factors of the atomic states. However, none of the previous studies have demonstrated the role of electron correlation effects explicitly arising through various physical effects in the determination of the total values of the g_j factors of the heavy atomic systems. Lindroth and Ynnerman have carried out such a rigorous investigation of the role of electron correlation effects in the corrections over the Dirac value of the g_j factors of the ground states in the Li, Be^+, and Ba^+ atomic systems, which have a valence electron in the s orbital. They employed a relativistic coupled-cluster (RCC) method and incorporated the Breit interaction in their calculations and found that higher-order correlation effects and the Breit interaction play significant roles in achieving precise results. However, they observed that lower-order contributions are still dominant in the evaluation of the corrections over Dirac value of the g_j factors. In particular, they observed that correlations due to all-order core-polarization effects, arising through a random-phase approximation type of diagrams, in these calculations are crucial. A number of calculations have reported very accurate values of this quantity using the multiconfiguration Dirac-Fock (MCDF) method highlighting the importance of including the higher excited configuration state functions (CSFs) for their determinations [7,18]. A shortcoming of this method is that it cannot explain the roles of different electron correlation effects explicitly except giving a qualitative idea of the importance of incorporating them to achieve precise results. Another point to be noted is that the MCDF method is a special case of the configuration-interaction (CI) method. It is known that a truncated CI method has problems with size consistency and size extensivity [19,20]. Moreover, in practice, only the important contributing CSFs are selected in this approach until the final results are achieved within the intended accuracies. In contrast, the truncated many-body methods formulated in the RCC theory framework are more capable of capturing the electron correlation effects rigorously than other existing atomic many-body methods and are also free from the size-extensivity and size-consistency problems owing to an exponential ansatz of the wave functions [19,20]. This is why RCC methods are generally referred to as golden tools for investigating the role of electron correlation effects in the spectroscopic studies. A number of properties in Ca^+ have been calculated by employing the RCC methods in the

*bijaya@prl.res.in

coupled-cluster with single- and double-excitation approximation (CCSD method) [9–12,21,22]. From these studies, the CCSD method and its equivalent level of approximated RCC methods are proven to be capable of giving very accurate results in the atomic systems having configurations similar to Ca^+. In fact, the g_j factor of the ground state of Ca^+ has been measured up to an accuracy of the seventh decimal place, which has also been supported by theory using the MCDF method [7]. Another measurement of the g_j factor in the $3d\,^2D_{5/2}$ state of this ion is reported up to sixth decimal precision [1]. However, there has not been any theoretical study carried out in this state to reproduce the experimental value. Thus, it would be interesting to evaluate g_j factors and learn the behavior of electron correlation effects in the ground and excited states of Ca^+. In the light of this interest, the present work is intended to carry out calculations of the g_j factors of the $4s\,^2S_{1/2}$, $4p\,^2P_{1/2}$, $4p\,^2P_{3/2}$, $3d\,^2D_{3/2}$, and $3d\,^2D_{5/2}$ states in the Ca^+ ion.

II. THEORY

The interaction Hamiltonian of an atomic electron when subjected to an external homogeneous magnetic field $\vec{\mathbf{B}}$ is given by [23]

$$H_{\rm mag} = ec\sum_i \vec{\boldsymbol{\alpha}}_i \cdot \vec{\mathbf{A}}_i = -\frac{ec}{2}\sum_i \vec{\boldsymbol{\alpha}}_i \cdot (\vec{\mathbf{r}}_i \times \vec{\mathbf{B}}), \tag{1}$$

where e is the electric charge of the electron, c is the speed of light, $\vec{\boldsymbol{\alpha}}$ is the Dirac operator, and $\vec{\mathbf{A}}$ is the vector field experienced by the electron located at r due to the applied magnetic field. This interaction Hamiltonian can be expressed in terms of a scalar product as

$$H_{\rm mag} = -\frac{ec}{2}\sum_i (\vec{\boldsymbol{\alpha}}_i \times \vec{\mathbf{r}}_i)\cdot\vec{\mathbf{B}} = i\frac{ec}{\sqrt{2}}\sum_i r_i\{\vec{\boldsymbol{\alpha}}_i \otimes \vec{\mathbf{C}}^{(1)}\}^{(1)}\cdot\vec{\mathbf{B}}, \tag{2}$$

with $C^{(1)}$ is the Racah coefficient of rank one.

Defining the above expression as $H_{\rm mag} = \vec{\mathcal{M}}\cdot\vec{\mathbf{B}}$ with magnetic moment operator $\vec{\mathcal{M}} = \sum_{i,q=-1,0,1}\vec{\boldsymbol{\mu}}_q^{(1)}(r_i)$, the Dirac value of the Landé g_j factor of a bound electron in an atomic system can be given by

$$g_j^D = -\frac{1}{\mu_B}\frac{\vec{\mathcal{M}}}{\vec{\mathbf{J}}}, \tag{3}$$

of a state with total angular momentum $\mathbf{J}$ for the Bohr magneton $\mu_B = e\hbar/2m_e$ with mass of electron m_e. Thus, the g_j^D value for the state $|JM\rangle$ can be evaluated using the projection theorem as

$$g_j^D = -\frac{1}{2\mu_B}\frac{\langle J\|\mathcal{M}\|J\rangle}{\sqrt{J(J+1)(2J+1)}}, \tag{4}$$

with the corresponding single-particle reduced matrix element of $\boldsymbol{\mu}^{(1)}$ given by

$$\langle\kappa_f\|\boldsymbol{\mu}^{(1)}\|\kappa_i\rangle = -(\kappa_f+\kappa_i)\langle -\kappa_f\|\mathbf{C}^{(1)}\|\kappa_i\rangle \times\int_0^\infty dr\, r(P_fQ_i + Q_fP_i), \tag{5}$$

where $P(r)$ and $Q(r)$ denote the large and small components of the radial parts of the single-particle Dirac orbitals, respectively, and the κ are their relativistic angular momentum quantum numbers. It can be noted here that this expression is similar to the expression for determining the magnetic dipole hyperfine structure constant; in both properties the angular momentum selection rule is restricted by the reduced matrix element of $C^{(1)}$, which is given as

$$\langle\kappa_f\|\mathbf{C}^{(k)}\|\kappa_i\rangle = (-1)^{j_f+1/2}\sqrt{(2j_f+1)(2j_i+1)} \times\begin{pmatrix} j_f & k & j_i \\ 1/2 & 0 & -1/2\end{pmatrix}\Pi(l_{\kappa_f},k,l_{\kappa_i}), \tag{6}$$

with

$$\Pi(l_{\kappa_f},k,l_{\kappa_i}) = \begin{cases}1 & \text{for } l_{\kappa_f}+k+l_{\kappa_i} \text{ even}\\ 0 & \text{otherwise}\end{cases} \tag{7}$$

for the orbital momentum l_κ of the corresponding orbital having the relativistic quantum number κ.

The net Landé g factor of a free electron (g_f) with the QED correction to the Dirac value (g_D) can be approximately evaluated as [24]

$$g_f \simeq g_D\times\left[1+\frac{1}{2}\frac{\alpha_e}{\pi}-0.328\left(\frac{\alpha_e}{\pi}\right)^2+\cdots\right] \approx 1.001\,160\times g_D, \tag{8}$$

where α_e is the fine-structure constant. From this analysis, the QED correction to the bound electron g_j factor can be estimated approximately by the interaction Hamiltonian as [25]

$$\Delta H_{\rm mag} \approx 0.001\,160\mu_B\beta\vec{\boldsymbol{\Sigma}}\cdot\vec{\mathbf{B}}, \tag{9}$$

where β and $\vec{\boldsymbol{\Sigma}}$ are the Dirac matrix and spinor, respectively. Following the above procedure, we can estimate the leading-order QED correction to g_j by defining an operator $\Delta\vec{\mathcal{M}} = \sum_{i,q=-1,0,1}\Delta\vec{\boldsymbol{\mu}}_q^{(1)}(r_i) = \sum_i\beta_i\vec{\boldsymbol{\Sigma}}_i$ such as [18]

$$\Delta g_j^Q = 0.001\,160\frac{\langle J\|\Delta\mathcal{M}\|J\rangle}{\sqrt{J(J+1)(2J+1)}}. \tag{10}$$

The corresponding reduced matrix element of the $\Delta\mu_q^{(1)}(r_i)$ is given by

$$\langle\kappa_f\|\Delta\boldsymbol{\mu}^{(1)}\|\kappa_i\rangle = (\kappa_f+\kappa_i-1)\langle -\kappa_f\|\mathbf{C}^{(1)}\|\kappa_i\rangle \times\int_0^\infty dr(P_fP_i + Q_fQ_i). \tag{11}$$

Hence, the total g_j value of an atomic state can be evaluated as $g_j = g_j^D + \Delta g_j^Q$ and can be compared with the experimental value wherever available.

III. METHODS FOR CALCULATIONS

The considered states of Ca^+ have a common closed core $[3p^6]$ of Ca^{2+} with a valence orbital from different orbital angular momenta and parity. We have developed a number of relativistic many-body methods and have been employing them to calculate wave functions of a variety of atomic systems including Ca^+ that have configurations as a closed core and a valence orbital [9,11,21,22,26,27]. Applications of these methods have proved that they are capable of giving rise to very accurate results comparable with the experimental values. We apply some of these methods considering various levels of approximations to demonstrate how these methods are incapable of producing precise values of the g_j factors in Ca^+. To determine the reason for the same, the role of correlation effects at the lower- and higher-order contributions is investigated systematically. Special efforts have been made to estimate contributions from the leading triply excited configurations in the RCC theory framework adopting perturbative approaches to carry out calculations in the available computational resources. For this purpose, we briefly discuss here the considered many-body methods and present results employing these methods to justify our above assessment.

To demonstrate various relativistic contributions systematically, we first perform calculations with the Dirac-Coulomb (DC) interaction and suppress contributions from the negative orbitals. In this approximation, the atomic Hamiltonian is given by

$$H^{\rm DC} = \sum_i \Lambda_i^+ [c\vec{\boldsymbol{\alpha}}_i \cdot \vec{\mathbf{p}}_i + (\beta_i - 1)c^2 + V_{\mathcal{N}}(r_i)]\Lambda_i^+ + \sum_{i,j>i} \Lambda_i^+ \Lambda_j^+ \frac{1}{r_{ij}} \Lambda_i^+ \Lambda_j^+, \tag{12}$$

where $V_{\mathcal{N}}(r)$ is the nuclear potential determined using the Fermi-charge distribution, $r_{ij} = |\vec{\mathbf{r}}_i - \vec{\mathbf{r}}_j|$ represents the interelectronic distance between the electrons located at i and j, and the Λ^+ operator represents a projection operator on the positive-energy orbitals. Worth mentioning here is that the negative-energy orbitals may contribute significantly, but it would be below the precision levels where the neglected electron correlation effects can also play dominant roles. This is why we have not put forth effort to account for these contributions in the present work.

It was found in the previous calculation for the ground state of Ca^+ that the frequency-independent Breit interaction contributes sizably for the evaluation of the g_j factor [7]. We also estimate contributions due to this interaction by adding the corresponding interaction potential energy expression in the atomic Hamiltonian as given by

$$V_B(r_{ij}) = -\frac{\{\vec{\boldsymbol{\alpha}}_i \cdot \vec{\boldsymbol{\alpha}}_j + (\vec{\boldsymbol{\alpha}}_i \cdot \hat{\mathbf{r}}_{ij})(\vec{\boldsymbol{\alpha}}_j \cdot \hat{\mathbf{r}}_{ij})\}}{2r_{ij}}, \tag{13}$$

where $\hat{\mathbf{r}}_{ij}$ is the unit vector along $\vec{r}_{ij}$.

Apart from estimating Δg_j^Q corrections to the g_j factors due to the QED effects, it can be expected that there would be corrections to the g_j^D values of the bound electrons from the modifications of the wave functions due to the QED effects. To estimate these corrections, we consider the lowest-order QED interactions due to the vacuum potential (VP) and self-energy (SE) effects in the calculations of the wave functions of the bound electrons. The VP is considered as the sum of the Uehling $[V_U(r)]$ and Wichmann-Kroll $[V_{\rm WK}(r)]$ potentials, while the SE potential is evaluated as the sum of the contributions from the electric and magnetic form factors as originally described in Ref. [28]. The considered expressions with the Fermi charge distribution were given explicitly in our previous work [27].

We first calculate the Dirac-Hartree-Fock (DHF) wave function of the $[3p^6]$ configuration ($|\Phi_0\rangle$) using the above interactions in the atomic Hamiltonian. Orbitals for the DHF wave function are obtained using the Gaussian-type orbitals that are given for Ca^+ elsewhere [22]. Then the DHF wave function of a state of Ca^+ is constructed as $|\Phi_v\rangle = a_v^\dagger|\Phi_0\rangle$ with the respective valence orbital v of the state. To show higher relativistic contributions explicitly, we perform calculations considering the DC Hamiltonian, then including the Breit interaction with the DC Hamiltonian, then with QED corrections in the DC Hamiltonian, and finally incorporating both the Breit and QED interactions simultaneously with the DC Hamiltonian. The reason for carrying out calculations considering individual relativistic corrections separately and then including them together is that we had observed in our previous study that sometimes correlations among the Breit and QED interactions alter the results more when they are incorporated independently.

To investigate the importance of electron correlation effects, we include them in both the lower-order and all-order many-body methods. In the lower-order approximations, we employ the relativistic second-order many-body perturbation theory [MBPT(2) method] and third-order many-body perturbation theory [MBPT(3) method]. In these approximations, we express the approximated atomic wave function as

$$|\Psi_v\rangle = \left(1 + \Omega_0^{(1)} + \Omega_v^{(1)}\right)|\Phi_v\rangle \tag{14}$$

in the MBPT(2) method and

$$|\Psi_v\rangle = \left(1 + \Omega_0^{(1)} + \Omega_v^{(1)} + \Omega_0^{(1)}\Omega_v^{(1)} + \Omega_0^{(2)} + \Omega_v^{(2)}\right)|\Phi_v\rangle \tag{15}$$

in the MBPT(3) method, where Ω_0 and Ω_v are known as wave operators. Here Ω_0 and Ω_v act over $|\Phi_0\rangle$ and $|\Phi_v\rangle$, respectively, to generate various CSFs in the perturbative approach. Amplitudes of these operators are determined by using the generalized Bloch's equations [29] as

$$\left\langle\Phi_0^*\middle|\left[\Omega_0^{(k)}, H_0\right]\middle|\Phi_0\right\rangle = \left\langle\Phi_0^*\middle|V_{es}\left(1 + \Omega_0^{(k-1)}\right)\middle|\Phi_0\right\rangle \tag{16}$$

and

$$\left\langle\Phi_v^*\middle|\left[\Omega_v^{(k)}, H_0\right]\middle|\Phi_v\right\rangle = \left\langle\Phi_v^*\middle|V_{es}\left(1 + \Omega_0^{(k-1)} + \Omega_v^{(k-1)}\right)\middle|\Phi_v\right\rangle - \sum_{m=1}^{k-1}\left\langle\Phi_v^*\middle|\Omega_v^{(k-m)}\middle|\Phi_v\right\rangle E_v^{(m)}, \tag{17}$$

where H_0 is the DHF Hamiltonian, $V_{es} = H - H_0$ is the residual potential, $|\Phi_0^*\rangle$ and $|\Phi_v^*\rangle$ are the excited configurations over the respective $|\Phi_0\rangle$ and $|\Phi_v\rangle$ DHF wave functions, and $E_v^{(k)} = \langle\Phi_v|V_{es}(1 + \Omega_0^{(k-1)} + \Omega_v^{(k-1)})|\Phi_v\rangle$ is the kth-order energy of the $|\Psi_v\rangle$ state.

After obtaining amplitudes of the MBPT operators, the g_j factors are calculated using the expression

$$\langle O\rangle = \frac{\langle\Psi_v|O|\Psi_v\rangle}{\langle\Psi_v|\Psi_v\rangle}, \tag{18}$$

where O stands for the respective $\mathcal{M}$ and $\Delta\mathcal{M}$ operators for the evaluations of the g_j^D and Δg_j^Q contributions, respectively. In a similar framework and using the exponential ansatz of RCC theory, atomic wave functions of the considered states with the respective valence orbitals are expressed as

$$|\Psi_v\rangle = e^T\{1+S_v\}|\Phi_v\rangle, \tag{19}$$

where T and S_v are the RCC operators that excite electrons from $|\Phi_0\rangle$ and $|\Phi_v\rangle$, respectively. We have approximated the RCC theory to only the single and double excitations (CCSD method). The single- and double-excitation processes carried out by these RCC operators are described by denoting these operators using the subscripts 1 and 2, respectively, as

$$T \simeq T_1 + T_2, \quad S_v \simeq S_{1v} + S_{2v}. \tag{20}$$

The amplitudes of these operators are evaluated by solving the equations

$$\langle\Phi_0^*|\overline{H}_N|\Phi_0\rangle = 0 \tag{21}$$

and

$$\langle\Phi_v^*|(\overline{H}_N - \Delta E_v)S_v|\Phi_v\rangle = -\langle\Phi_v^*|\overline{H}_N|\Phi_v\rangle, \tag{22}$$

where $|\Phi_0^*\rangle$ and $|\Phi_v^*\rangle$ are excited up to doubles, $\overline{H}_N = (H_N e^T)_l$ represents for the linked terms only with the normal-order Hamiltonian $H_N = H - \langle\Phi_0|H|\Phi_0\rangle$, and ΔE_v is the attachment energy for the state $|\Psi_v\rangle$, which is determined by

$$\Delta E_v = \langle\Phi_v|\overline{H}_N\{1+S_v\}|\Phi_v\rangle. \tag{23}$$

To investigate the role of the electron correlation effects through the nonlinear terms in the RCC theory, we also perform calculations considering only linear terms in the single- and double-excitation approximation in this theory (which is termed the LCCSD method). In this approximation, it yields

$$|\Psi_v\rangle \approx \{1+T+S_v\}|\Phi_v\rangle, \tag{24}$$

$$\overline{H}_N \approx H_N + H_N T, \tag{25}$$

and

$$\overline{H}_N S_v \approx H_N + H_N T + H_N S_v. \tag{26}$$

After obtaining amplitudes of the RCC operators, the expectation values as in Eq. (18) are evaluated as

$$\frac{\langle\Psi_v|O|\Psi_v\rangle}{\langle\Psi_v|\Psi_v\rangle} = \frac{\langle\Phi_v|\{1+T^\dagger+S_v^\dagger\}O\{1+T+S_v\}|\Phi_v\rangle}{\langle\Phi_v|\{1+T^\dagger+S_v^\dagger\}\{1+T+S_v\}|\Phi_v\rangle} \tag{27}$$

in the LCCSD method and

$$\frac{\langle\Psi_v|O|\Psi_v\rangle}{\langle\Psi_v|\Psi_v\rangle} = \frac{\langle\Phi_v|\{1+S_v^\dagger\}e^{T^\dagger}Oe^T\{1+S_v\}|\Phi_v\rangle}{\langle\Phi_v|\{1+S_v^\dagger\}e^{T^\dagger}e^T\{1+S_v\}|\Phi_v\rangle} \tag{28}$$

in the CCSD method. Clearly, the expression for the LCCSD method gives rise to a finite number of terms like in the MBPT(2) and MBPT(3) methods. However, the expression for the CCSD method has two nonterminating series in the numerator and denominator as $e^{T^\dagger}Oe^T$ and $e^{T^\dagger}e^T$, respectively. These nontruncative series give a large number of nonlinear terms corroborating a large space of CSFs belonging to higher level of excitations. To account for contributions from both the nontruncative series, we adopt iterative procedures. This is done by performing calculations through intermediate steps, in which we compute and store first the $O + OT + T^\dagger O + T^\dagger OT$ terms from $e^{T^\dagger}Oe^T$ and $1 + T^\dagger T$ terms from $e^{T^\dagger}e^T$. Then we operate a T operator and subsequently a $T^\dagger$ operator in the above intermediate calculations and replace them as the new intermediate calculations. This procedure is repeated until we attain contributions up to 10^{-8} precision level convergence in the values from the higher nonlinear terms.

As we will see, the correlation effects coming through the CCSD terms give much larger magnitudes to the g_j factors than the available experimental values for the ground [7] and $3d\,^2D_{5/2}$ [1] states of Ca^+, even though this method was proven to give reasonably accurate results for a number of properties in the considered ion as stated in the Introduction. To find out how the higher level excitations would circumvent this to bring back the results close to the experimental values, we define RCC operators in a perturbative framework to account for contributions from the important triply excited configurations from both $|\Phi_0\rangle$ and $|\Phi_v\rangle$ as

$$T_3^{\rm pert} = \frac{1}{6}\sum_{abc,pqr}\frac{(H_N T_2)_{abc}^{pqr}}{\epsilon_a+\epsilon_b+\epsilon_c-\epsilon_p-\epsilon_q-\epsilon_r} \tag{29}$$

and

$$S_{3v}^{\rm pert} = \frac{1}{4}\sum_{ab,pqr}\frac{(H_N T_2 + H_N S_{2v})_{abv}^{pqr}}{\Delta E_v+\epsilon_a+\epsilon_b-\epsilon_p-\epsilon_q-\epsilon_r}, \tag{30}$$

where $\{a,b,c\}$ and $\{p,q,r\}$ represent for the occupied and virtual orbitals, respectively, and the ϵ are their single-particle orbital energies. Contributions from the $T_3^{\rm pert}$ and $S_{3v}^{\rm pert}$ operators to the g_j factors are estimated using Eq. (28) by considering them as part of the T and S_v operators. In this approach, we evaluate extra terms $T_2^\dagger O T_3^{\rm pert}$, $T_2^\dagger O S_{3v}^{\rm pert}$, $S_{2v}^\dagger O S_{3v}^{\rm pert}$, $S_{1v}^\dagger T_2^\dagger O S_{3v}^{\rm pert}$, $T_3^{\rm pert\dagger} O T_3^{\rm pert}$, $S_{3v}^{\rm pert\dagger} O S_{3v}^{\rm pert}$, and their complex conjugate (c.c.) terms. These terms are computationally very expensive and give more than 500 Goldstone diagrams, but are found to be crucial in achieving reasonably accurate results compared to the available experimental values.

IV. RESULTS AND DISCUSSION

In order to gauge correctness of the wave functions obtained by employing many-body methods at different levels of approximations, we first present electron attachment energies to the considered states of Ca^+ in Table I and compare them with the experimental values listed in the National Institute of Science and Technology (NIST) database [30]. We consider only the $4s\,^2S_{1/2}$, $3d\,^2D_{3/2}$, $3d\,^2D_{5/2}$, $4p\,^2P_{1/2}$, and $4p\,^2P_{3/2}$ states of Ca^+ as the representative states with different angular momentum and parity for our investigation. As can be seen from this table, the DHF results differ significantly from the experimental values, while the MBPT(2) values are larger than

TABLE I. Electron attachment energies (in cm^{-1}) using relativistic many-body methods at different levels of approximations with the DC Hamiltonian. Higher-order relativistic corrections from the Breit interaction and QED effects are quoted from the CCSD method considering them separately and including them together (given in the row labeled "Breit + QED"). Our final CCSD results are compared with the experimental values (in the row "Expt.") listed in the NIST database [30].

Method	$4s\,^2S_{1/2}$	$3d\,^2D_{3/2}$	$3d\,^2D_{5/2}$	$4p\,^2P_{1/2}$	$4p\,^2P_{3/2}$
DHF	91439.97	72617.49	72593.39	68036.82	67837.16
MBPT(2)	96542.41	83943.81	83372.99	71026.03	70654.06
LCCSD	96737.80	84564.90	84397.55	71101.05	70862.78
CCSD	95879.60	81695.19	81606.44	70603.50	70372.14
			Relativistic corrections		
Breit	−7.42	37.98	53.15	−11.02	−3.70
QED	−5.68	2.11	2.52	0.02	0.66
Breit + QED	−13.09	40.08	55.67	−11.01	−3.05
Total	95866.51	81735.27	81662.11	70592.49	70369.09
Expt.	95751.87(3)	82101.68	82040.99	70560.36	70337.47

the experimental results. The LCCSD method does not seem to improve the calculations and give even larger values than the MBPT(2) results. However, the CCSD method reduces these results close to the experimental values. Corrections from the Breit and QED interactions are given separately in the same table from the CCSD method. They are also estimated by including both these interactions simultaneously. In this case, we find that the sum of the individual corrections and simultaneous account for these corrections, given as Breit + QED in the above table, give almost the same contributions. In our earlier work on the Cs atom, we had found similar behavior for the attachment energies but different trends were exhibited in the evaluation of the transition properties [27]. Nevertheless, the higher-order relativistic corrections also remove slightly the discrepancies among the CCSD results and experimental values of the energies. It may be possible that the omitted contributions from the triple excitations improve the CCSD values further.

After understanding the role of the electron correlation effects in the evaluation of the energies, we present the calculated g_j values of the $4s\,^2S_{1/2}$, $3d\,^2D_{3/2}$, $3d\,^2D_{5/2}$, $4p\,^2P_{1/2}$, and $4p\,^2P_{3/2}$ states of Ca^+ in Table II from a number of methods approximated at different levels. This also includes all the methods that were considered to evaluate energies along with the MBPT(3) method, which involves energies from the MBPT(2) method. To highlight how the correlation effects propagate in these methods, we present results systematically from lower-order to all-order LCCSD and CCSD methods. Final results are given as the CCSD values along with the corrections from the approximated triple excitations along with the uncertainties. Uncertainties are estimated mainly by extrapolating contributions due to modifications of wave functions of the CCSD method through the triple excitations. We present both the g_j and Δg_j^Q results from the DHF method in the beginning to appraise beforehand how much the electron correlation effects may contribute to yielding results close to the experimental values in the measured states. If we are able to achieve results agreeing with the experimental values for some states then it may be possible to predict these values for other states using the employed many-body methods where measurements are not carried out. From the analysis of the behavior of the correlation effects in the determination of the attachment energies, it was obvious to us that there were large differences between the calculations obtained using the DHF method and the experimental values. When we compare the net g_j values of the ground and $3d\,^2D_{5/2}$ states, after adding up the g_j^D and Δg_j^Q values, with the experimental results [1,7] quoted at the end of the above table, it gives the impression that the electron correlation effects may not play a strong role in attaining calculated values matching with the experimental results. So it is natural to assume that employment of a lower-order method can suffice the purpose. In an experimental paper on the ground-state result, theoretical results were also presented by carrying out a rigorous calculation employing the MCDF method [7]. It was demonstrated there that a very large configurational space was required to attain results matching with their measured value. It was also highlighted in that work that the Breit interaction contribution was essential in achieving a high-precision theoretical result.

As we move on, we will explain the reasons why it is strenuous to achieve results below the 10^{-5} precision level by employing the RCC theory in the CCSD method approximation. Thus, we prefer to not present the calculated values of the g_j factors beyond the sixth decimal places here. The necessity of including higher-level excitations through the RCC method to improve these results further is demonstrated by investigating contributions from the leading-order triple-excitation contributions involving the core and valence orbitals in the MBPT(3) method and in the perturbative approach using the RCC operators as defined in Eqs. (29) and (30). We have also provided corrections to g_j from the Breit and QED corrections, considering them separately and also considering both interactions together. The estimated Δg_j^Q corrections from the CCSD method are also listed explicitly. The signs of these corrections are not the same for all the states owing to the $\kappa_f + \kappa_i - 1$ factor in Eq. (11). It is obvious from Table II that our CCSD results match only up to the third decimal place with the available experimental values of the ground and $3d\,^2D_{5/2}$ states. Trends can also be noted from this work in the results starting from the DHF method to the CCSD method: Values from different approximated methods are vacillating in all the states.

TABLE II. Demonstration of trends of the calculated g_j values in various relativistic methods using the DC Hamiltonian. Relativistic corrections from the Breit and QED interactions using the CCSD method and contributions from the important triple excitations (triples) are given separately. The estimated Δg_j^Q contributions of the DHF and CCSD methods are also listed within the parentheses to learn about their typical magnitudes. The final values along with the uncertainties are compared with the available experimental results for the $4s\ ^2S_{1/2}$ and $3d\ ^2D_{5/2}$ states.

Method	$4s\ ^2S_{1/2}$	$3d\ ^2D_{3/2}$	$3d\ ^2D_{5/2}$	$4p\ ^2P_{1/2}$	$4p\ ^2P_{3/2}$
		DC contributions of the DHF method			
DHF	2.002273	0.798994	1.200845	0.665090	1.334854
(Δg_j^Q)	(0.002320)	(−0.000464)	(0.000464)	(−0.000773)	(0.000773)
		DC contributions to g_j from lower-order methods			
MBPT(2)	2.001871	0.798176	1.197682	0.665684	1.333777
MBPT(3)	2.002313	0.781590	1.186383	0.669046	1.334676
LCCSD	1.999070	0.800532	1.198077	0.665901	1.333605
		CCSD results for g_j from different interactions			
DC	2.002703	0.799047	1.200895	0.665912	1.334294
DC + Breit	2.002700	0.799085	1.200903	0.665916	1.334295
DC + QED	2.002703	0.799085	1.200903	0.665916	1.334295
DC + Breit + QED	2.002700	0.799085	1.200903	0.665917	1.334295
DC + Breit + QED + triples	2.002267	0.798554	1.200341	0.665636	1.333861
(Δg_j^Q)	(0.002321)	(−0.000465)	(0.000465)	(−0.000773)	(0.000773)
Final	2.002267(30)	0.798554(25)	1.200341(30)	0.665636(15)	1.333861(25)
Experiment	2.00225664(9) [7]		1.2003340(25) [1]		

Since the differences among the values of the g_j factors from various methods are very small, the role of electron correlation effects is not realized distinctly. To make it more pronounced, we plot the $(g_j^D - \text{DHF})/(g_j - \text{DHF})$ values considering g_j^D values from different methods in Fig. 1 for all the states. The trends of the electron correlation effects incorporated in these methods are highlighted. As can be seen from this figure, the correlation contributions do not follow a definite trend and they are quite significant in view of achieving high-precision values. Also, we give contributions

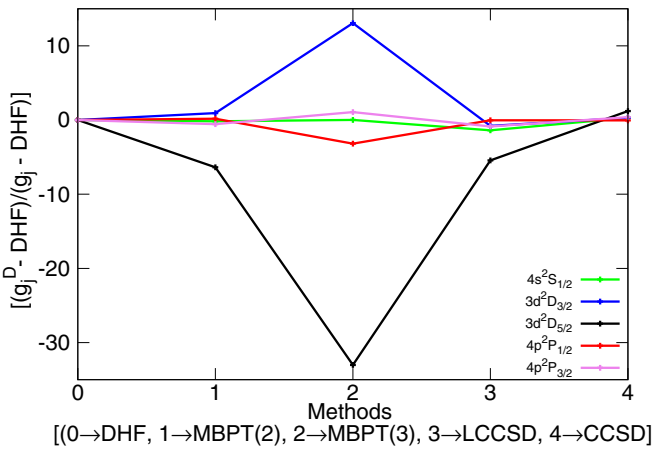

FIG. 1. Trends of electron correlation effects among the $4s\ ^2S_{1/2}$, $3d\ ^2D_{3/2}$, $3d\ ^2D_{5/2}$, $4p\ ^2P_{1/2}$, and $4p\ ^2P_{3/2}$ states for the evaluation of g_j^D values in Ca^+. We plot the relative $(g_j^D - \text{DHF})/(g_j - \text{DHF})$ values to highlight the roles of correlation effects through different many-body methods. We consider values from the DHF, MBPT(2), MBPT(3), LCCSD, and CCSD methods in a sequence on the X axis in an arbitrary unit distance.

to the g_j values for all the considered states from the individual terms of the CCSD method including the terms involving the perturbed triple-excitation operators in Table III. This is to show how some of the higher-order terms in the all-order perturbative method contribute more than the lower-order RCC terms. The DHF value gives here the largest contribution as it includes the Dirac g_D value. It has been found in earlier studies on hyperfine-structure constants and quadrupole moments of atomic states in $^{43}Ca^+$ using the RCC method [11] that after the DHF value, the dominant contributions come from the OS_{1v} and OS_{2v} terms along with their c.c. terms due to the electron correlation effects. It should be kept in mind that the OS_{1v} term accounts for the lowest-order electron pair-correlation effects, while the OS_{2v} term incorporates the lowest-order electron core-polarization effects in the RCC framework [31,32]. The other terms encompass higher-order correlation effects due to nonlinearity in the RCC operators. Hence, it is generally anticipated that the contributions from these nonlinear terms are relatively small compared to the above two terms. However, as seen here, many of the nonlinear terms give much larger contributions, almost by an order, than the lower-order RCC terms. Significantly contributing correlation effects are given in bold in Table III. Those nonlinear terms from the CCSD method are not listed in the table; their total contributions are given in the row labeled "Extra". It is obvious from this table that these contributions are quite large, especially in the $3d\ ^2D_{5/2}$ state, which has been underlined. This suggests that the core correlation contributions appearing through the T operators in the nonlinear terms play active roles in the evaluation of the g_j values. Thus, it supports the consideration that a perturbative method would completely fail to estimate the g_j factors accurately in an atomic system. We have also seen in Table II that contributions from the estimated triple excitations through the perturbed RCC operators are the

TABLE III. Contributions from individual CCSD terms to the g_j^D values in the $4s\,^2S_{1/2}$, $3d\,^2D_{3/2}$, $3d\,^2D_{5/2}$, $4p\,^2P_{1/2}$, and $4p\,^2P_{3/2}$ states. Contributions given in the rows labeled "Extra" and "Norm" are obtained from the rest of the nonlinear terms of the CCSD method that are not listed here and corrections due to normalization of the wave functions, respectively. Values up to only the sixth decimal place are given and those values are finite but contribute below 10^{-6} precision level are quoted as ∼0.0. Unusually large contributions from the correlation effects are given in bold. We have also underlined the "Extra" contribution to the $3d\,^2D_{5/2}$ state to draw attention to its very large value.

RCC terms	$4s\,^2S_{1/2}$	$3d\,^2D_{3/2}$	$3d\,^2D_{5/2}$	$4p\,^2P_{1/2}$	$4p\,^2P_{3/2}$
O	1.999953	0.799922	1.199917	0.666636	1.333308
OT_1 + c.c.	∼0.0	0.0	0.0	∼0.0	∼0.0
$T_1^\dagger O T_1$	0.000001	0.0	0.0	0.000003	0.000007
$T_1^\dagger O T_2$ + c.c.	∼0.0	0.0	0.0	∼0.0	∼0.0
$T_2^\dagger O T_2$	**−0.000912**	**−0.006104**	**−0.009066**	−0.000234	−0.000525
OS_{1v} + c.c.	−0.000009	−0.000016	−0.000018	−0.000003	−0.000005
OS_{2v} + c.c.	0.000001	−0.000004	0.000005	−0.000003	−0.000003
$T_1^\dagger O S_{2v}$ + c.c.	**−0.000984**	**−0.001526**	**−0.002282**	−0.000144	−0.000284
$T_2^\dagger O S_{2v}$ + c.c.	∼0.0	∼0.0	∼0.0	∼0.0	∼0.0
$S_{1v}^\dagger O S_{1v}$	**0.005060**	**0.009181**	**0.013637**	**0.001606**	**0.003169**
$S_{1v}^\dagger O S_{2v}$+c.c.	∼0.0	∼0.0	0.000001	∼0.0	∼0.0
$S_{2v}^\dagger O S_{2v}$	**0.016159**	**0.018597**	0.000008	**0.004210**	**0.007462**
$T_2^\dagger O T_3^{\rm pert}$ + c.c.	∼0.0	∼0.0	∼0.0	∼0.0	∼0.0
$S_{2v}^\dagger O T_3^{\rm pert}$ + c.c.	0.0	0.0	0.0	0.0	0.0
$T_2^\dagger O S_{3v}^{\rm pert}$ + c.c.	**−0.001650**	**−0.000907**	**−0.001104**	**−0.000440**	**−0.000804**
$S_{2v}^\dagger O S_{3v}^{\rm pert}$ + c.c.	∼0.0	∼0.0	∼0.0	∼0.0	∼0.0
$T_3^{\rm pert\dagger} O T_3^{\rm pert}$	**0.000136**	**0.000159**	**0.000235**	0.000050	0.000098
$S_{3v}^{\rm pert\dagger} O S_{3v}^{\rm pert}$	**0.000728**	**0.000238**	**0.000366**	**0.000130**	**0.000255**
$S_{1v}^\dagger T_2^\dagger O S_{3v}^{\rm pert}$ + c.c.	−0.000076	−0.000021	−0.000007	−0.000021	−0.000038
Extra	**0.002951**	**−0.001207**	**0.026959**	**−0.000313**	**0.000411**
Norm	−0.021567	−0.019331	−0.028730	−0.005073	−0.010019

decisive factors in attaining the results close to the available experimental values. Following the perturbative analysis, it can be perceived that the $T_2^\dagger O T_3^{\rm pert}$, $S_{2v}^\dagger O T_3^{\rm pert}$, $T_2^\dagger O T_3^{\rm pert}$, and $S_{2v}^\dagger O S_{3v}^{\rm pert}$ RCC terms account for the lowest-order terms involving the triply excited perturbed excitation operators. Since the $S_{3v}^{\rm pert}$ operator involves the valence orbital, the term including this operator usually gives larger contributions than the counterterms with the $T_3^{\rm pert}$ operator. However, a comparison between the contributions obtained through the $T_2^\dagger O T_3^{\rm pert}$, $S_{2v}^\dagger O S_{3v}^{\rm pert}$, and $S_{3v}^{\rm pert\dagger} O S_{3v}^{\rm pert}$ terms in Table III suggest that the correlation contributions do not manifest this trend. Analyzing in terms of level of excitations associated with all these operators, as defined in Ref. [19], it can be understood that the Goldstone diagrams involving the particle-particle and hole-hole excitations through the $\mathcal{M}$ operator are important physical processes and the hole-particle and particle-hole excitations do not play much of a role in determining the g_j values.

Again, we have observed that similar types of Goldstone diagrams exhibit completely different trends of correlation effects for the lowest-order and all-order methods. To demonstrate this more prominently, we find the leading-order contributing diagrams from the $T_2^\dagger O T_3^{\rm pert}$ and $S_{2v}^\dagger O S_{3v}^{\rm pert}$ RCC terms and compare the contributions from these diagrams with their corresponding lowest-order Goldstone diagrams appearing through the MBPT(3) method. We have shown some of these diagrams in Fig. 2 and quote their contributions in Table IV from the MBPT(3) and RCC methods. As can be

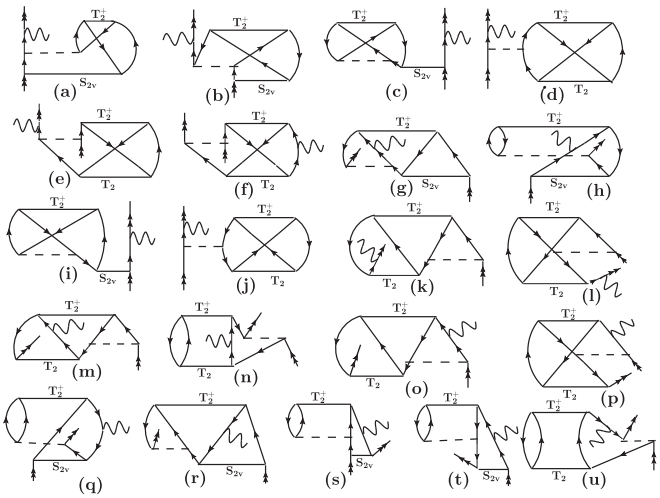

FIG. 2. Some of the important contributing Goldstone diagrams appearing through the $T_2^\dagger O S_{3v}^{\rm pert}$ RCC term. Lines going up and down represent the virtual and occupied orbitals of Ca^+. Lines with double arrows correspond to the valence orbital, dashed horizontal lines denote Coulomb interaction, and solid horizontal lines correspond to the all-order Coulomb interactions appearing through the T_2 and S_{2v} operators.

TABLE IV. Contributions to g_j^D values of different states from the individual diagrams shown in Fig. 2. Values are given after multiplying with 10^3 to highlight their contributions prominently and those values that are unusually large are in bold. This clearly demonstrates the importance of considering an all-order perturbative method for the determination of the g_j factors in the atomic systems.

	$4s\,^2S_{1/2}$		$3d\,^2D_{3/2}$		$3d\,^2D_{5/2}$		$4p\,^2P_{1/2}$		$4p\,^2P_{3/2}$	
Diagram	MBPT(3)	RCC	MBPT(3)	RCC	MBPT(3)	RCC	MBPT(3)	RCC	MBPT(3)	RCC
Fig. 2(a)	0.4425	**0.9141**	0.3852	**0.8401**	0.5758	**1.2575**	0.0874	0.1820	0.1732	0.3613
Fig. 2(b)	−0.1108	−0.1652	−0.1864	−0.2811	−0.2800	−0.4228	−0.03306	−0.0565	−0.0668	−0.1143
Fig. 2(c)	0.2023	0.3247	0.4086	0.6099	0.6107	0.9123	0.0426	0.0742	0.0848	0.1477
Fig. 2(d)	**12.6380**	**20.5263**	**7.7036**	**12.2213**	**11.5434**	**18.3284**	**3.5011**	**5.5020**	**6.9796**	**10.9658**
Fig. 2(e)	−0.2017	−0.2983	−0.5771	−0.9463	−0.8665	−1.4226	−0.03446	−0.0488	−0.0689	−0.0976
Fig. 2(f)	−0.2015	−0.2976	0.7874	1.3197	0.0436	0.0882	0.0518	0.0766	−0.0256	−0.0344
Fig. 2(g)	−0.0913	−0.1323	0.0596	0.0845	−0.0843	−0.1372	0.0060	0.0090	−0.0385	−0.0670
Fig. 2(h)	0.2316	0.3907	−0.1859	−0.2984	0.0250	0.0662	0.0088	0.0027	0.0939	0.1601
Fig. 2(i)	−0.2204	−0.3402	−0.4415	−0.6485	−0.6600	−0.9701	−0.0459	−0.0770	−0.0915	−0.1533
Fig. 2(j)	**−12.7009**	**−20.6074**	**−7.8297**	**−12.3756**	**−11.7321**	**−18.5594**	**−3.5141**	**−5.5182**	**−7.0057**	**−10.9981**
Fig. 2(k)	0.1408	0.2022	**0.5118**	**0.8461**	**0.7691**	**1.2728**	0.0270	0.0350	0.0544	0.0709
Fig. 2(l)	0.1322	0.1910	**0.4986**	**0.8294**	**0.74897**	**1.2473**	0.0256	0.0332	0.0516	0.0672
Fig. 2(m)	0.1403	0.2013	**−0.8225**	**−1.3819**	−0.1216	−0.2143	−0.0442	−0.0620	0.0183	0.0213
Fig. 2(n)	−0.4488	−0.6347	0.0055	0.0536	−0.9322	−1.2610	−0.0238	−0.0225	−0.1680	−0.2248
Fig. 2(o)	0.1409	0.2023	**0.5057**	**0.8341**	**0.7651**	**1.2648**	0.0024	0.0315	0.05293	0.0692
Fig. 2(p)	0.1323	0.1911	**0.4847**	**0.8071**	**0.7399**	**1.2323**	0.0202	0.0268	0.0489	0.0641
Fig. 2(q)	−0.2309	−0.4032	0.1170	0.1908	−0.0707	−0.1466	0.0206	0.0371	−0.0793	−0.1334
Fig. 2(r)	0.0914	0.1369	−0.0665	−0.1048	0.0801	0.1306	−0.0237	−0.0471	0.0294	0.0501
Fig. 2(s)	0.0962	0.1688	−0.0104	−0.0180	0.0496	0.0379	−0.0289	−0.0342	−0.0012	−0.0093
Fig. 2(t)	0.0087	**0.2768**	−0.0025	−0.0058	−0.0032	0.0927	0.0023	−0.00553	0.0018	**−0.0784**
Fig. 2(u)	0.4482	0.6543	−0.1303	−0.1868	**0.8479**	**1.2160**	−0.0046	−0.0068	0.1536	0.2175

seen from this table, there are huge differences in some of the results obtained from the MBPT(3) method and from the level of RCC calculations. Several contributions are shown in bold to call attention to the unusually large contributions at the lower- and all-order level calculations. Again, it is obvious from this table that some diagrams contribute predominantly to the lower angular momentum states while other diagrams contribute significantly in higher angular momentum states. Some changes in the correlation trends are also observed among the states belonging to different parities.

Nonetheless, unusually large contributions arising through the perturbed triple-excitation RCC operators imply that the RCC theory in the CCSD method approximation is not capable of producing values below 10^{-5} precision of the g_j factors in Ca^+. Also, contributions arising through some of the nonlinear terms that are higher than the linear terms in the CCSD method suggest that consideration of full triple excitations may be imperative to achieve g_j factors below the above precision level. Moreover, either estimating the $g_j^D - g_D$ value as in Ref. [15] or developing alternative RCC theories, such as biorthogonal RCC theory [19], to avoid the appearance of nontruncative series as in Eq. (28) to determine the g_j factor of a state in this ion would be inevitable.

V. CONCLUSION

We have employed a number of relativistic many-body methods to investigate role of the electron correlation effects in the determination of the g_j factors of the first five low-lying atomic states in the singly charged calcium ion. To validate these methods, we presented the electron attachment energies by employing these methods and compared them against the experimental values listed in the National Institute of Science and Technology database. This demonstrated the gradual improvement in the accuracy of the results from lower many-body methods to the all-order relativistic coupled-cluster method with the single- and double-excitation approximation. However, when these methods were employed for the determination of the g_j factors of the considered atomic states, the trends of the correlation effects were found to be very peculiar in nature. In fact, the results obtained employing the mean-field theory in the Dirac-Hartree-Fock approach were found to be in better agreement with the experimental values than the lower-order many-body perturbation theories and relativistic coupled-cluster theory approximation with linear terms. We also found that triple-excitation contributions are the decisive factors in achieving very precise values for the g_j factors and their contributions through the lower-order and all-order correlation effects behave in a completely different way. Nonetheless, the overall observation from this study is that it is very challenging to attain highly accurate g_j factors (below 10^{-5} precision) in many-electron systems by employing a truncated many-body method as the contributions from the electron correlation effects do not converge with the higher-order approximations. Thus, it is reliable to determine the $g_j - g_D$ value instead of the net g_j value of an atomic state. Also, it is imperative to develop more powerful relativistic many-body methods circumventing the problem of appearing nontruncative series so that trends of the correlation effects can be systematically investigated and calculations can be improved gradually in the determination of the g_j factors in a many-electron atomic system. Since unique correlation effects

are associated with the determination of g_j factors, it suggests that a relativistic many-body method can be indeed scrutinized by producing high-precision values for these factors in heavy atomic systems. This test would be of immense interest in a number of applications such as investigating parity nonconservation and frequency standard studies in atomic systems more reliably.

ACKNOWLEDGMENTS

B.K.S. acknowledges financial support from CAS through a PIFI Fellowship under Project No. 2017VMB0023. This work was partly supported by the TDP project of the Physical Research Laboratory (PRL), Ahmedabad and the computations were carried out using the Vikram-100 HPC cluster of PRL.

[1] M. Chwalla, J. Benhelm, K. Kim, G. Kirchmair, T. Monz, M. Riebe, P. Schindler, A. S. Villar, W. Hänsel, C. F. Roos, R. Blatt, M. Abgrall, G. Santarelli, G. D. Rovera, and P. Laurent, Phys. Rev. Lett. **102**, 023002 (2009).
[2] Y. Huang, J. Cao, P. Liu, K. Liang, B. Ou, H. Guan, X. Huang, T. Li, and K. Gao, Phys. Rev. A **85**, 030503(R) (2012).
[3] M. Riebe, H. Häffner, C. F. Roos, W. Hänsel, J. Benhelm, G. P. T. Lancaster, T. W. Körber, C. Becher, F. Schmidt-Kaler, D. F. V. James, and R. Blatt, Nature (London) **429**, 734 (2004).
[4] T. P. Harty, D. T. C. Allcock, C. J. Ballance, L. Guidoni, H. A. Janacek, N. M. Linke, D. N. Stacey, and D. M. Lucas, Phys. Rev. Lett. **113**, 220501 (2014).
[5] C. J. Ballance, T. P. Harty, N. M. Linke, M. A. Sepiol, and D. M. Lucas, Phys. Rev. Lett. **117**, 060504 (2016).
[6] T. Pruttivarasin, M. Ramm, S. G. Porsev, I. I. Tupitsyn, M. S. Safronova, M. A. Hohensee, and H. Häffner, Nature (London) **517**, 592 (2015).
[7] G. Tommaseo, T. Pfeil, G. Revalde, G. Werth, P. Indelicato, and J. P. Desclaux, Eur. Phys. J. D **25**, 113 (2003).
[8] W. M. Itano, Phys. Rev. A **73**, 022510 (2006).
[9] B. K. Sahoo, M. R. Islam, B. P. Das, R. K. Chaudhuri, and D. Mukherjee, Phys. Rev. A **74**, 062504 (2006).
[10] D. Jiang, B. Arora, and M. S. Safronova, Phys. Rev. A **78**, 022514 (2008).
[11] B. K. Sahoo, Phys. Rev. A **80**, 012515 (2009).
[12] M. S. Safronova and U. I. Safronova, Phys. Rev. A **83**, 012503 (2011).
[13] Y.-B. Tang, H.-X. Qiao, T.-Y. Shi, and J. Mitroy, Phys. Rev. A **87**, 042517 (2013).
[14] C. Shi, F. Gebert, C. Gorges, S. Kaufmann, W. Nörtershäuser, B. K. Sahoo, A. Surzhykov, V. A. Yerokhin, J. C. Berengut, F. Wolf, J. C. Heip, and P. O. Schmidt, Appl. Phys. B **123**, 2 (2017).
[15] E. Lindroth and A. Ynnerman, Phys. Rev. A **47**, 961 (1993).
[16] A. V. Volotka, D. A. Glazov, V. M. Shabaev, I. I. Tupitsyn, and G. Plunien, Phys. Rev. Lett. **112**, 253004 (2014).
[17] V. M. Shabaev, D. A. Glazov, G. Plunien, and A. V. Volotka, J. Phys. Chem. Ref. Data **44**, 031205 (2015).
[18] K. T. Cheng and W. J. Childs, Phys. Rev. A **31**, 2775 (1985).
[19] I. Shavitt and R. J. Bartlett, *Many-Body Methods in Chemistry and Physics* (Cambridge University Press, Cambridge, 2009).
[20] A. Szabo and N. Ostuland, *Modern Quantum Chemistry*, 1st ed. (Dover, Mineola, 1996).
[21] C. Sur, K. V. P. Latha, B. K. Sahoo, R. K. Chaudhuri, B. P. Das, and D. Mukherjee, Phys. Rev. Lett. **96**, 193001 (2006).
[22] B. K. Sahoo, B. P. Das, and D. Mukherjee, Phys. Rev. A **79**, 052511 (2009).
[23] J. J. Sakurai, *Advanced Quantum Mechanics* (Addison-Wesley, Reading, 1967).
[24] A. Czarnecki, U. D. Jentschura, K. Pachucki, and V. A. Yerokhin, Can. J. Phys. **84**, 453 (2006).
[25] A. J. Akhiezer and V. B. Berestetskii, *Quantum Electrodynamics* (Interscience, New York, 1965), Chap. 8, Sec. 50.2.
[26] D. K. Nandy and B. K. Sahoo, Phys. Rev. A **90**, 050503(R) (2014).
[27] B. K. Sahoo, Phys. Rev. A **93**, 022503 (2016).
[28] V. V. Flambaum and J. S. M. Ginges, Phys. Rev. A **72**, 052115 (2005).
[29] I. Lindgren and J. Morrison, *Atomic Many-Body Theory*, 2nd ed. (Springer, Berlin, 1986).
[30] http://physics.nist.gov/PhysRefData/ASD/levels_form.html
[31] B. K. Sahoo, G. Gopakumar, R. K. Chaudhuri, B. P. Das, H. Merlitz, U. S. Mahapatra, and D. Mukherjee, Phys. Rev. A **68**, 040501(R) (2003).
[32] B. K. Sahoo, S. Majumder, R. K. Chaudhuri, B. P. Das, and D. Mukherjee, J. Phys. B **37**, 3409 (2004).